DESIGN OF PROTOTYPE FILTER FOR NEAR-PERFECT-RECONSTRUCTION OVERLAPPED COMPLEX-MODULATED TRANSMULTIPLEXERS

Shahriar Mirabbasi and Ken Martin
Department of Electrical and Computer Engineering
University of Toronto
Toronto, Ontario, M5S 3G4, Canada

ABSTRACT

A simple method for the design of the finite-impulse-response prototype filter for maximally-decimated overlapped complex modulated transmultiplexers with near perfect reconstruction property is presented. The procedure is unified for all values of overlap factor and leads to a prototype filter with excellent frequency selectivity and fast side-lobe fall-off rate. The high stop-band attenuation and fast side-lobe fall-off rate, which is justified analytically, make the proposed filters suitable candidates for high-speed data communication applications employing multicarrier modulation.

1. INTRODUCTION

Multicarrier modulation is an efficient technique for transmitting information, especially broadband data, over wireline and wireless channels. This modulation scheme can be described in the context of filter bank based transmultiplexers (TMUXs) [1][2][3][4][5]. In efficient contemporary implementations of multicarrier modulation, known as discrete multitone modulation (DMT) or orthogonal frequency division multiplexing (OFDM), modulation and demodulation are performed digitally using the inverse discrete Fourier transform (IDFT) and the DFT. However, given a practical communication channel, the significant spectral overlap between signalling filters in a DFT-based filter bank (side-lobes on the order of -13 dB) results in performance degradation of the system [4][6][7]. For example, a narrowband interference in a frequency band could effect several subchannels and make them unusable.

To alleviate the problems associated with the poor frequency selectivity of subchannel filters in DFT-based multitone systems, alternative filter-bank-based techniques such as the overlapped DMT or the discrete wavelet multitone (DWMT) are proposed [4][6][7]. These filter banks use finite-impulse-response (FIR) filters of length greater than that of rectangular filters in DFT-based systems and result in better subchannel spectral containment, without sacrificing the Nyquist properties of the set of subchannel waveforms. Better stop-band attenuation and subchannelization results in both lower levels of interchannel interference (ICI) and greater robustness to narrow-band interference [4][7]. For an M-channel system, the length of the subchannel filters is typically gM with $g>1$ (as opposed to $g=1$ in conventional DMT systems). Thus, the pulse waveforms for different symbol blocks overlap in time and hence g is called the overlap-factor.

In realizing these alternative filter-bank-based TMUXs, depending on the application (complex or real base-band signal models), complex-modulated or cosine-modulated filter banks are used. In these types of filter banks, synthesis and analysis filters are typically derived from a prototype filter; therefore, the number of parameters to be optimized is small compared to a general filter bank. Moreover, efficient implementation techniques exists for both complex- or cosine-modulated filter banks [4][8].

In this paper, we consider the case of a complex-modulated TMUX

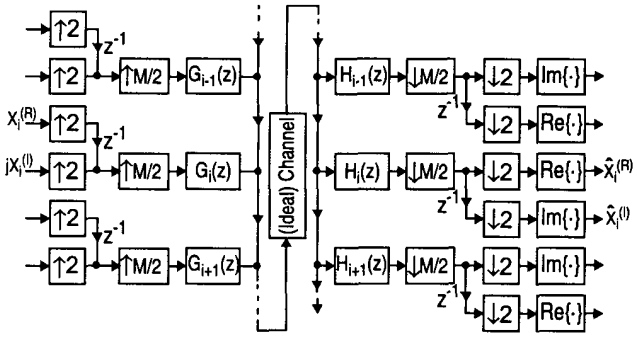

Figure 1 Modified DFT transmultiplexer

in which the subchannel filters have possibly complex coefficients. To achieve filters with real coefficients, standard methods such as combining two filters in the synthesis (or analysis) bank which have complex conjugate coefficients, similar to techniques used in cosine-modulated filter banks [8][10] can be employed.

Also, we focus on a TMUX system with near perfect reconstruction (NPR) property (assuming an ideal channel). As mentioned in [1] and [6] it is often judicious to relax the PR condition by allowing small amplitude and aliasing (cross-talk) distortion, while achieving the better stop-band performance (increased frequency selectivity) of sub-channel filters. The NPR TMUX system that we consider is a variation of the modified DFT (MDFT) TMUX [9][10] which will be briefly reviewed in Section 2. The design procedure for the prototype filter with good stop-band fall-off performance is discussed in Section 3 where the fast fall-off rate of the designed filter spectrum is justified analytically.

2. MDFT TRANSMULTIPLEXERS

An MDFT transmultiplexer [9][10] is shown in Figure 1 in which the number of channels M is assumed to be even. In this system all the filters in the filter bank are derived from an FIR baseband prototype filter with frequency response $P(e^{j\omega})$ by complex modulation:

$$G_i(e^{j\omega}) = M \cdot P(e^{j(\omega-(2\pi i)/M)}) \qquad i = 0, 1, \ldots, M-1 \quad (1)$$

$$H_i(e^{j\omega}) = P(e^{j(\omega-(2\pi i)/M)}) \qquad i = 0, 1, \ldots, M-1 \quad (2)$$

It is called a modified DFT TMUX because of the following additional modifications to the DFT filter bank [10]: the real and imaginary parts of the input and output signals to the TMUX are staggered by the offset of $M/2$ and the assignment of real and imaginary parts to the inputs and outputs of each channels alternates from channel to channel as illustrated in Figure 1.

It can be shown [9][10] that the overall MDFT TMUX system has a structure inherent alias (cross-talk) cancellation, i.e. the cross-talk between adjacent channels is cancelled. The remaining

0-7803-7448-7/02/$17.00 ©2002 IEEE

cross-talk between non-adjacent subchannels can be kept arbitrarily small by appropriate design of the prototype filter (and its stop-band attenuation). A prototype filter with good spectral containment in which the stop-band attenuation increases for greater frequency differences from its passband edge would minimize the cross-talk. The design of a class of such prototype filter is the subject of this paper.

Before presenting the prototype design it is worth mentioning that as suggested in [6] the synthesis and analysis filters of a MDFT TMUX can be constructed from a prototype filter as follows:

$$G_i(e^{j\omega}) = j^i \cdot P(e^{j(\omega-(2\pi i)/M)}) \qquad i = 0, 1, \ldots, M-1 \quad (3)$$

$$h_i(n) = g_i^*(N-n) \quad (4)$$

In (4) N is the length of prototype filter and * represents complex conjugation. The inclusion of the factor j^i in the synthesis (transmit) filters does not change the magnitude of their frequency response; it is equivalent to and in lieu of alternating the assignment of real and imaginary parts of the inputs and outputs in the MDFT TMUX.

3. PROTOTYPE DESIGN

In this work, we assume that the prototype filter belongs to a class of low-pass filters with the general form of:

$$p(n) = k_0 + 2\sum_{l=1}^{g-1} k_l \cos\left(\frac{2\pi ln}{N}\right) \qquad 0 \le n < N \quad (5)$$

where $N=gM$. Here the overlap factor g is a positive integer and M is the number of channels in the TMUX system. Note that the prototype filter introduced in [6] has the same general form as in equation (5). Also notice that the well-known Hamming, Hanning and Blackman windows are special cases of this prototype low-pass filter [11], i.e., with k_0=0.5 and $2k_1$=-0.5 (k_0=0.54 and $2k_1$=-0.46), $p(n)$ represents the Hanning (Hamming) window and with k_0=0.42, $2k_1$=-0.50 and $2k_2$=0.08, $p(n)$ realizes the Blackman window.

We will now discuss the requirements on the coefficients k_l ($0 \le l < g$) which in addition to providing a good stop-band performance of the channel filters, results in a near-perfect reconstruction property of the TMUX:

Let us temporarily ignore the causality requirements, then a low-pass filter of the form:

$$w(n) = c_0 + 2\sum_{l=1}^{g-1} c_l \cos\left(\frac{2\pi ln}{N}\right) \qquad -\frac{N}{2} \le n < \frac{N}{2} \quad (6)$$

with $c_l > 0$ (for $0 \le l < g$) and $N=gM$, has even-symmetry and therefore is a linear phase filter. A filter of this form can achieve a good stop-band performance as well as a fast side-lobe fall-off rate [11][12]. Furthermore, as will be discussed later, with a proper choice of coefficients c_l, the -3 dB bandwidth of this filter would be π/M with the main-lobe width of $2\pi/M$ [6]. We construct our prototype filter from a causal version of the FIR low-pass filter of equation (6), that is, by shifting the time index by $N/2$ samples, i.e., $p(n)=w(n-N/2)$ where

$$w\left(n-\frac{N}{2}\right) = c_0 + 2\sum_{l=1}^{g-1} c_l \cos\left(\frac{2\pi ln}{N} - \pi l\right) \qquad 0 \le n < N \quad (7)$$

$$= c_0 + 2\sum_{l=1}^{g-1} (-1)^l c_l \cos\left(\frac{2\pi ln}{N}\right) \qquad 0 \le n < N \quad (8)$$

Comparing the right-hand sides of equations (5) and (8) we have:

$$k_l = (-1)^l c_l \qquad 0 \le l < g \quad (9)$$

Since $c_l > 0$ (for $0 \le l < g$), (9) indicates that the adjacent coefficients of the prototype filter should have alternating signs with k_0 being positive. This fact was heuristically justified in [6].

Next we discuss the conditions on k_l (for $0 \le l < g$) required for $p(n)$ to have a fast fall-off rate of its side-lobes. For continuous-time functions, it is known that the smoother a function is, as measured by the number of continuous derivatives it possesses, the more compact is its Fourier transform; that is, the faster its transform dies away with increasing frequency. In fact, if a continuous-time function and its first n-1 derivatives are continuous, its Fourier transform dies away at least as rapidly as $|\Omega|^{-(n+1)}$ for large Ω (Ω being the frequency in rad/sec) [13].

Although this theorem has also been used for the case of discrete-time windows [11], special care should be given to applying the theorem to discrete-time functions. The subtle point is in the interpretation of continuity and existence of derivatives for discrete-time functions. However, if a discrete-time function is a sampled version of a smooth continuous-time function with a high enough sampling rate, then assuming the Fourier transform of the underlying continuous-time function dies away at least as rapidly as $|\Omega|^{-(n+1)}$, the rate of fall-off of the side-lobes of the corresponding sampled (discrete-time) function would be approximately $|\omega|^{-(n+1)}$ ($\omega=\Omega T$ is the scaled discrete-time frequency and T is the sampling period). The justification for this statement is as follows:

It is well-known [14] that if $p(n)$ is a sampled version of continuous-time function $p_c(t)$ with sampling-period T, i.e., $p(n) = p_c(nT)$, then the following relation holds between the discrete-time Fourier transform $P(e^{j\omega})$ and Fourier transform $P_c(j\Omega)$.

$$P(e^{j\omega}) = \frac{1}{T}\sum_{m=-\infty}^{\infty} P_c\left(j\Omega - \frac{2\pi m}{T}\right)\Bigg|_{\Omega=\frac{\omega}{T}} \quad (10)$$

Thus, $P(e^{j\omega})$ consists of periodically repeated copies of the frequency-scaled version of $P_c(j\Omega)$ with the period $\Omega_s=2\pi/T$. This is illustrated in Figure 2. The larger the sampling-frequency (or equivalently the smaller the sampling-period T), the more the periodic components of $P(e^{j\omega})$ are separated in frequency domain. Thus, as can be seen from the figure, by increasing the sampling frequency, the effect of the aliasing in the spectrum of $P(e^{j\omega})$ which is due to overlapping of the tails of adjacent copies of $P_c(j\Omega)$, becomes less significant. Hence, the rate of fall-off of $P(e^{j\omega})$ more closely resembles that of $P_c(j\Omega)$ (Figure 2(b)).

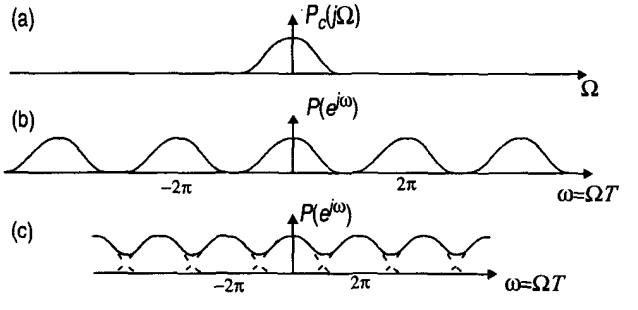

Figure 2 (a) Spectrum of a continuous-time signal, along with spectra of sampled versions of it when sampling rate ($1/T$) is (b) higher or (c) lower than Nyquist rate.

In our case, the prototype filter is a sampled version of the following continuous-time function:

$$p_c(t) = \begin{cases} k_0 + 2\sum_{l=1}^{g-1} k_l \cos(l\Omega_N t) & 0 \le t \le NT \\ 0 & otherwise \end{cases} \quad (11)$$

where $\Omega_N = 2\pi/(NT)$ and T is the sampling period.

With a proper choice of coefficients k_l (for $0 \le l < g$), the Fourier transform of $p_c(t)$ has a -3 dB bandwidth of $\Omega \approx \pi/(MT)$ and main-lobe width of $\Omega \approx 2\pi/(MT)$ with $M=N/g$ [6]. Hence, by sampling $p_c(t)$ with the sampling period of T, we are in fact oversampling $p_c(t)$ by roughly a factor of $M/2$. As a result, the effect of aliasing in the discrete-time Fourier transform of $p(n) = p_c(nT)$ become less significant, specially as M (and thus oversampling factor) becomes larger. Consequently, if the Fourier transform of $p_c(t)$ falls of at the rate of $|\Omega|^{-(n+1)}$, then the fall-off rate of discrete Fourier transform of $p(n)$ would be $|\omega|^{-(n+1)}$.

Furthermore, the cosine functions in the summation of equation (11) are continuous and so are all their derivatives, except perhaps at the boundary points: $t = 0$ and $t=NT$. Hence, the only points that need to be considered for the purpose of smoothness of this function are the boundary points. Due to the symmetry of $p_c(t)$, i:e., $p_c(t) = p_c(t\text{-}NT)$ for $0 \le t \le NT$, it suffices to check for the continuity of the function and its derivatives only at the boundary point $t = 0$.

Note that because of the special form of $p_c(t)$, its odd order derivatives are already continuous at the boundary points. This is because:

$$p_c^{(r)}(t) = \begin{cases} 2\sum_{l=1}^{g-1} (-1)^{\alpha} (l\Omega_N)^r k_l \sin(l\Omega_N t) & 0 \le t \le NT \\ 0 & otherwise \end{cases} \quad (12)$$

where $p_c^{(r)}(t)$ is the r-th order derivative of $p_c(t)$ with respect to t and r is an odd positive integer. The integer number α is a function of r and its value is immaterial for the purpose of our discussion. As can be seen from equation (12), at the boundary point $t=0$, any odd-order derivative of $p_c(t)$ is continuous and $p_c^{(r)}(0) = 0$.

Thus, for a positive and even integer number q, if the q-th order derivative of $p_c(t)$ at boundary point $t=0$ is continuous, then the Fourier transform of $p_c(t)$ falls off at the rate of at least $|\Omega|^{-(q+3)}$. This is due to the fact that the $(q+1)$-th order derivative would be continuous as well (since $q+1$ would be an odd number). As explained earlier, this implies that the fall-off rate of discrete Fourier transform of $p(n)$ would be approximately $|\omega|^{-(q+3)}$.

Now let us discuss the conditions required for continuity of $p_c(t)$ and its even-order derivatives. For $p_c(t)$ to be continuous at $t=0$ (or equivalently its 0-th order derivative to be continuous), we need $p_c(0)=0$. Considering equation (11) this requires:

$$k_0 + 2\sum_{l=1}^{g-1} k_l = 0 \quad (13)$$

This requirement was also heuristically justified in [6]. Note that if (13) is satisfied then the side-lobes of discrete Fourier transform of $p(n)$ would have the approximate fall-off rate of $|\omega|^{-3}$. This fall-off rate is significantly faster than the fall-off rate of filters in standard DFT based TMUXs, which due to the use of rectangular windowing have fall-off rate of $|\omega|^{-1}$.

For an even integer q (with $q \ge 2$) the qth-order derivative of $p_c(t)$ has the form:

$$p_c^{(q)}(t) = \begin{cases} 2\sum_{l=1}^{g-1} (-1)^{\beta} (l\Omega_N)^q k_l \cos(l\Omega_N t) & 0 \le t \le NT \\ 0 & otherwise \end{cases} \quad (14)$$

where the integer number β is a function of q and its value is inconsequential for the purpose of our discussion. In order for $p_c^{(q)}(t)$ to be continuous at $t=0$ we should have $p_c^{(q)}(0) = 0$ which requires:

$$2\sum_{l=1}^{g-1} (l\Omega_N)^q k_l = 0 \qquad q \ge 2 \quad (15)$$

Equation (15) can be simplified to:

$$\sum_{l=1}^{g-1} l^q k_l = 0 \qquad q \ge 2 \quad (16)$$

As discussed earlier, if equation (16) holds for even-integer number q then the fall-off rate of $P(e^{j\omega})$ would be approximately $|\omega|^{-(q+3)}$.

So far we have focused on the conditions required on the coefficients k_l, such that the spectrum of the prototype filter $p(n)$ has a fast fall-off rate (good stop-band performance). To have a (near) PR complex-modulated TMUX, the prototype filter should have the (approximate) power-complementary property [6][8][10]:

$$\sum_{m=1}^{M-1} \left| P(e^{j(\omega - (2\pi m)/M)}) \right|^2 = c \quad (17)$$

where c is a positive constant. Without loss of generality, we can assume that $c=1$. It can be shown [6], that equation (17) is approximately satisfied if coefficients k_l are chosen such that:

$$\begin{cases} k_0 = 1 \\ k_l^2 + k_{g-l}^2 = 1 \qquad l = 1, 2, \ldots, \left\lfloor \frac{g}{2} \right\rfloor \end{cases} \quad (18)$$

Here $\lfloor x \rfloor$ represents the largest integer that is less than or equal to x. If coefficients k_l are chosen such that equations in (18) hold, the -3 dB frequency of the prototype filter would be π/M [6].

Given the overlap-factor g, in order to realize the prototype filter we need to find the g coefficients k_l (for $0 \le l < g$). In general, we need a system of g (independent) equations to solve for g coefficients k_l. Equations (13) and (18) account for $\lfloor g/2 \rfloor + 2$ equations. Equation (16) can be used to construct the remainder of the equations necessary to have a system of g equations. The system of equations contains quadratic equations (because of (18)), and in general might have more than one set of solutions. An acceptable solution would satisfy the constraint that the adjacent coefficients of the prototype filter should have alternating signs with $k_0=1$ (due to (18)). The values of example prototype filter coefficients for $3 \le g \le 8$ are tabulated in Table 1. Note that, for $g>4$ the coefficient values are different from those reported in [6]. Also, note that the proposed procedure for finding the coefficients is unified for any value of g and is based on solving a system of g equations g unknowns. This is further simplification compared to the method of [6] which for $g>4$ is based on an iterative optimization procedure.

The minimum stop-band attenuation(MSA) and the minimum rate of fall-off (MRF) of the side-lobes of $P(e^{j\omega})$ for different values of g is also given in Table 1. The MSA was found to be only a function of the overlap factor g and independent of the filter order. The MRF can be determined based on the number of equations that are generated using (13) and (16) to find the coefficient values. For example, for g=5, (18) and (13) provide us with four equations and the last equation is obtained from (16) using q=2. This implies that the approximate fall-off rate of $P(e^{j\omega})$ is $|\omega|^{-5}$.

Also listed in Table 1 are the signal-to-noise ratios (SNRs) of an 8-channel MDFT TMUX with the proposed prototype filter for different values of g. In calculating SNR, the only noise considered is reconstruction error, i.e., errors due to aliasing (cross-talk) and inter-channel interference at the TMUX output. The inputs to the TMUX are random complex numbers whose real and imaginary parts are uniformly distributed between -1 and 1. As can be seen, the distortion due to reconstruction error is very small and negligible in most practical multicarrier applications [1][6] and decreases as g increases.

As a final example, the spectra of the proposed prototype filter and that of [6] (with g=8 and N=64) for an 8-channel MDFT TMUX are shown in Figure 3. Also shown in the figure is the line with a fall-off rate proportional to $|\omega|^{-7}$. As expected, the fall-off rate of the proposed filter for large frequencies is faster than $|\omega|^{-7}$. Also, as can be seen from the figure the fall-off rate of the proposed filter is faster than that of same order filter of [6] although its first side-lobe is higher. This result is typical for other values of g. It should be noted that the fall-off rate of the filters proposed in [6] was shown to be superior than that of other filters such as those in [7].

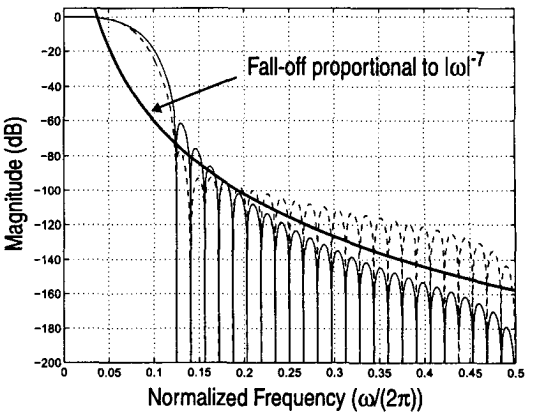

Figure 3 Spectra of the proposed prototype filter (solid-line) and that of reference [6] (dashed-line) for g=8 and N=64.

4. CONCLUSION

A simple procedure for the design of a highly selective prototype filter for overlapped complex-modulated NPR TMUXs is presented. The design method is unified for all values of the overlap factor. The minimum stop-band attenuation and the minimum fall-off rate of the side-lobes of the filter is found to be a function of the overlap factor and independent of the filter order. The fast side-lobe fall-off rate of the designed filter is justified analytically and is superior to that of previously reported FIR filters for filter-bank applications.

coefficients	*g=3*	*g=4*	*g=5*	*g=6*	*g=7*	*g=8*
k_0	+1.00000000	+1.00000000	+1.00000000	+1.00000000	+1.00000000	+1.00000000
k_1	-0.91143783	-0.97195983	-0.99184131	-0.99818572	-0.99938080	-0.99932588
k_2	+0.41143783	+0.70710678	+0.86541624	+0.94838678	+0.97838560	+0.98203168
k_3		-0.23514695	-0.50105361	-0.70710678	-0.84390076	-0.89425129
k_4			+0.12747868	+0.31711593	+0.53649931	+0.70710678
k_5				-0.06021021	-0.20678881	-0.44756522
k_6					+0.03518546	+0.18871614
k_7						-0.03671221
MSA (dB)	32.58	39.86	48.25	58.12	63.45	61.54
MRF	$\|\omega\|^{-3}$	$\|\omega\|^{-3}$	$\|\omega\|^{-5}$	$\|\omega\|^{-5}$	$\|\omega\|^{-7}$	$\|\omega\|^{-7}$
SNR (dB)	49.21	68.31	69.88	89.34	90.09	104.58

Table 1: Coefficients of the prototype filter for different values of g, along with the minimum stop-band attenuation (MSA) and minimum rate of fall-off (MRF) of the side-lobes and SNR of the 8-channel MDFT TMUX based on the prototype filter.

5. REFERENCES

[1] A. Viholainen, T. Saramäki, and M. Renfors, "Nearly Perfect-Reconstruction Cosine-Modulated Filter Bank Design For VDSL Modems," Proceedings of The 6th IEEE ICECS, Sep. 1999, Vol. 1, pp.373-376.

[2] A.N. Akunsu, P. Duhamel, X. Lin, and M. de Courville, "Orthogonal Transmultiplexers in Communications: A Review," *IEEE Trans. on SP*, vol. 46, April 1998, pp. 979-995.

[3] P.P. Vaidyanathan, "Filter Banks in Digital Communications," *IEEE CAS Magazine*, 2001, vol. 1, no. 2 , pp. 4-25.

[4] S. Govardhanagiri, T. Karp, P. Heller, and T. Nguyen, "Performance Analysis of Multicarrier Modulation Systems Using Cosine Modulated Filter Banks," Proceedings of IEEE ICASSP, 1999, vol. 3, pp. 1405-1408.

[5] T. Ihalainen, J. Alhava, A. Viholainen, H. Xing, J. Rinne, and M. Renfors, "On the Performance of Filter Bank Based Multicarrier Systems in xDSL and WLAN Applications," Proceedings of IEEE ICC-2000, vol. 2, pp. 1120-1124.

[6] K.W. Martin, "Small Side-Lobe Filter Design for Multitone Data-Communication Applications," *IEEE TCAS-II*, vol. 45, no. 8, Aug. 1998, pp. 1155-1161.

[7] S.D. Sandberg and M.A. Tzannes, "Overlapped Discrete Multitone Modulation for High Speed Copper Wire Communications," *IEEE JSAC*, vol. 13, no. 12, Dec. 1995, pp. 1571-1585.

[8] P.P. Vaidyanathan, *Multirate Systems and Filter Banks*, Prentice Hall, Englewood Cliffs, NJ, 1993.

[9] G. Rösel and N.J. Fliege, "Transmultiplexer Filter Banks with Extremely Low Crosstalk and Intersymbol Interference," Proceedings of IEEE ISCAS, 1995, vol. 2, pp. 1448-1451.

[10] N.J. Fliege, *Multirate Digital Signal Processing*, John Wiley & Son, New York, NY, 1999.

[11] F.J. Harris, "On the Use of Windows for Harmonic Analysis with the Discrete Fourier Transform," *Proceedings of the IEEE*, vol. 66, no. 1, Jan. 1978, pp. 51-83.

[12] A.H. Nuttall, "Some Windows with Very Good Sidelobe Behavior," *IEEE Trans. on ASSP*, vol. 29, Feb. 1981, pp. 84-91.

[13] R.N. Bracewell, *The Fourier Transform and Its Applications*, McGraw-Hill, Boston, MA, 2000.

[14] A.V. Oppenheim, R.W. Schafer with J.R. Buck, *Discrete-Time Signal Processing*, Prentice-Hall, Upper Saddle River, NJ, 1999.